Available online at www.sciencedirect.com
SCIENCE DIRECT®
Journal of Hydrology 319 (2006) 96–108
Journal of Hydrology
www.elsevier.com/locate/jhydrol

Effective scaling factor for transient infiltration in heterogeneous soils

Jianting Zhu[a,*], Binayak P. Mohanty[b,1]

[a]Desert Research Institute, Division of Hydrologic Sciences, 755 E Flamingo Road, Las Vegas, NV 89119, USA
[b]Biological and Agricultural Engineering Department, 301C Scoates Hall, Texas A&M University, College Station, TX 77843-2117, USA

Received 7 April 2004; revised 24 June 2005; accepted 7 July 2005

Abstract

Effective hydraulic properties at large grid resolution are viable alternatives to heterogeneous soil medium in large-scale hydrologic and global circulation models. In this study, we investigate the effective hydraulic parameters for transient infiltration under ponding conditions in terms of the optimal averaging schemes for the input hydraulic and environmental parameter fields. The main idea of effective parameters is whether the interested process behavior in heterogeneous soils can be captured by a process that assumes only one set of soil parameters, such that the heterogeneous system is replaced by an equivalent homogeneous system. The 'effective' hydraulic parameters of the heterogeneous soil formation are derived by conceptualizing that the 'effective' homogeneous soil will approximately discharge the ensemble-mean surface flux and cumulative infiltration. The derived optimal effective powers for the random (input) parameters define an optimal averaging scheme for the random input fields, which can be used in large-scale hydrologic and global circulation models. Specifically, we discuss the effects of microtopography (as reflected in surface ponding depth), and hydraulic parameter correlation on the ensemble-mean behavior as well as on the optimal effective powers. For a large range of hydraulic properties from silty clay to sand with large uncertainties in the Miller–Miller scaling factor, the saturated water content, and the surface ponding depth, relatively small range of optimal effective power values has been found. Among the three, variability of the Miller–Miller scaling factor has the most significant effect on the ensemble flux behavior. The correlation among the Miller–Miller scaling factor, the saturated water content and the surface ponding depth increases the effects of soil heterogeneity. However, the ensemble-mean flux behavior can be more precisely mimicked through the idea of optimal effective powers when the random fields are better correlated.

Keywords: Heterogeneity; Unsaturated zone; Scaling factor; Infiltration; Soil–water balance.

1. Introduction

The variably saturated vadose zone determines the partitioning of rainfall over surface runoff and infiltration and the partitioning of infiltrated water over evapotranspiration and groundwater recharge.

* Corresponding author. Tel.: +1 702-862-5416; fax: +1 702-862-5427.
E-mail addresses: jianting.zhu@dri.edu (J. Zhu), bmohanty@tamu.edu (B.P. Mohanty).
[1] Tel.: +1 979 458 4421; fax: +1 979 845 3932.

0022-1694/$ - see front matter © 2005 Elsevier Ltd All rights reserved.
doi:10.1016/j.jhydrol.2005.07.004

Because the soil hydraulic characteristics that determine unsaturated flow exhibit a large degree of spatial heterogeneity, the surface water storage, the infiltration rate, the evapotranspiration rate, and the recharge rates vary correspondingly. Furthermore, representation of spatial variabilities of these processes and parameters is a complex problem because of the nonlinearity of the unsaturated flow equation. In an early work, Sharma and Luxmoore (1979) revealed the complexities of soil-plant-atmospheric interactions in evaluating the influence of soil variability on water balance. They indicated that the results were highly dependent on the coefficient of variation and the frequency distribution function of the Miller–Miller scaling factor, and the soil–plant–weather combination. More recently, Kim and Stricker (1996) employed Monte Carlo simulation to investigate the separate and simultaneous effects of horizontal heterogeneity of soil hydraulic properties and rainfall intensity on various statistical properties of the components of the one-dimensional water budget. Their results showed that the heterogeneity of soil hydraulic properties on the components of the annual water budget has a stronger effect for loam than for sand. Kim et al. (1997) further investigated the impact of heterogeneity of the soil hydraulic property on the spatially averaged water budget of the unsaturated zone based on an analytical framework (Kim et al., 1996). According to a previous study for the steady state unsaturated flow problems (Zhu and Mohanty, 2002); there are no universal effective properties due to highly nonlinear nature of soil hydraulic properties and various boundary conditions. Furthermore, they demonstrated that the effective parameters for infiltration and evaporation could be quite different under different flow scenarios.

This study is a more focused effort on transient infiltration under surface ponding condition and also considers the influence of variability of the surface ponding depth. We investigate the 'effective' (equivalent) soil hydraulic properties in terms of uncertainties of the hydraulic parameters coupled with the effects of microtopography. The main idea of effective parameters is whether the interested process behavior in heterogeneous soils can be captured by a process that assumes only one set of soil parameters, such that the heterogeneous system is replaced by an equivalent homogeneous system. The set of parameters that define the equivalent homogeneous system are referred to as effective parameters for the system. 'Equivalent' soil hydraulic properties should closely produce the same water budget as the mean water budget corresponding to a random field of soil hydraulic properties and the variation of microtopography. Although the idea of 'effective' or 'equivalent' soil has been suggested and studied quite extensively (e.g. Montoglou and Gelhar, 1987a–c; Unlu et al., 1990; Ferrante and Yeh, 1999), many previous studies have been done in the deeper and unbounded vadose zone where the idea of effective hydraulic parameters can be used more successfully. This study aims to study the near-surface vadose zone flow processes that are critical for hydro-climatic and land-atmosphere interaction modeling. It is generally agreed that the 'effective' parameters either can be difficult to define or should depend on the flow scenario we are interested in (e.g. Milly and Eagleson, 1987; Kim and Stricker, 1996; Kim et al., 1997). In this study, we adopt the power average for the hydraulic parameters and try to find the optimal average schemes as 'effective parameters' in an attempt to offer some guidelines of hydraulic parameter averaging scheme in dealing with infiltration in a large heterogeneous field under surface ponding conditions. The optimal p is the power that should be used in order to best simulate the ensemble behavior of heterogeneous soils. In other words, the optimal p is the power, which defines a best average scheme under the flow scenario considered. We investigate the horizontal spatial variability of soil behavior by using the Monte Carlo technique. Parallel non-interacting stream-tubes with one-dimensional models have been used as an approximation for various simplified vertical flow problems. Our study focuses on the case where the variability is in the horizontal plane. For example, in meso-scale Soil–Vegetation–Atmosphere Transfer (SVAT) schemes used in hydro-climatic models, pixel dimensions may range several hundred square meters to several hundred square kilometers, while the vertical scale of subsurface processes is limited to top few meters only. In such a large horizontal scale, the horizontal heterogeneity of hydraulic properties dominates. Therefore, it is reasonable to consider only the horizontal heterogeneity of soils for such an application. This implies that the soil behaves as bundle of

parallel stream tubes without lateral interaction, although the hydraulic properties may correlate across the stream tubes. This approach has been proven to be quite accurate for typical field dimensions for steady state infiltration and evaporation (Zhu and Mohanty, 2002).

2. Local scale infiltration equations

We use an implicit equation developed by Haverkamp et al. (1990) for one-dimensional infiltration subject to a head-type boundary condition. The formula has the same dimensionless form as that derived by Parlange et al. (1985), but it includes a new parameter, h_{str}, that may be conceptualized as the bubbling pressure or the air entry value in the soil moisture characteristic curve evident near saturation (e.g. Brooks and Corey, 1964). Haverkamp et al. (1990) considered two limiting cases of clayey and sandy soils and found that the formula produced accurate predictions of infiltration. Therefore, the formula is expected to be applicable to most soil types. The formula for infiltration that expresses the cumulative infiltration, I, as a function of time, t, through the water flux at the soil surface q_s, is as follows (when the surface ponding depth, h_{surf}, is not related to t)

$$I(t)-K_i t=(h_{surf}+h_{str})\frac{K_s(\theta_s-\theta_i)}{q_s-K_s}+\frac{S^2-2h_{str}K_s(\theta_s-\theta_i)}{2(K_s-K_i)}\ln\left(1+\frac{(K_s-K_i)}{(q_s-K_s)}\right) \quad (1)$$

and

$$t=\frac{K_s(h_{surf}+h_{str})(\theta_s-\theta_i)}{(q_s-K_s)(K_s-K_i)}-\frac{S^2-2h_{str}K_s(\theta_s-\theta_i)}{2(K_s-K_i)(q_s-K_i)}+\frac{S^2-2K_s(\theta_s-\theta_i)(h_{surf}+h_{str})}{2(K_s-K_i)^2}\ln\left(1+\frac{(K_s-K_i)}{(q_s-K_s)}\right) \quad (2)$$

where θ_s and θ_i are the saturated and the initial moisture content, respectively; K_s and K_i are the hydraulic conductivities at saturated and the initial moisture content, respectively; and S is the sorptivity.

The above solution of Richards equation for one-dimensional, isothermal water flow in unsaturated homogeneous and isotropic soil applies under the following initial and boundary conditions

$$\theta=\theta_i \quad \text{for } t=0 \quad \text{and } z>0 \quad (3)$$

$$\theta=\theta_s \quad \text{for } t\geq 0 \quad \text{and } z=0 \quad (4)$$

where z is depth positive downward.

3. Heterogeneous soils

Many previous investigation of soil heterogeneity often assumed so-called scaling heterogeneity (Sharma and Luxmoore, 1979; Jury et al., 1987; Hopmans et al., 1988; Russo, 1991; Kim and Stricker, 1996; Mayer and Miller, 1996; Kim et al., 1997). Scaling theory, based on the similar media concept (Miller and Miller, 1956), provides a basis for representing soil spatial variability in terms of a single stochastic variable, the scaling factor, which is related to the microscopic characteristic length of the soil. Two soils are considered to be similar when they only differ with respect to their internal microscopic geometries. In other words, it is assumed that the heterogeneity in the soil hydraulic properties is represented by a scaling factor, which is considered as being a realization of a spatial stochastic function. We adopt the macroscopic Miller similitude by Sposito and Jury (1985) and use the relative saturation ($\theta_{rel}=\theta/\theta_s$) as the water content parameters in scaling relationships. The heterogeneity in the relative saturation, θ_{rel}, the hydraulic conductivity, K and the sorptivity, S can be represented by spatially distributed scaling functions (e.g. Miller, 1980; Jury et al., 1987)

$$\theta_{rel}=\theta^*_{rel} \quad (5)$$

$$K(\theta_{rel},x,y)=K^*(\theta_{rel})\delta^2(x,y) \quad (6)$$

$$S(\theta_{rel},x,y)=S^*(\theta_{rel})\delta^{1/2}(x,y) \quad (7)$$

where θ_{rel}, K, and S are the scaled values at location (x, y) in two-dimensional case. θ^*_{rel}, K^*, and S^* denote values at a reference location.

In this study, we use the van Genuchten–Mualem model to represent the soil hydraulic properties

$$S_e[1+(\alpha\psi)^n]^{-m} \tag{8}$$

$$K = K_s S_e^{1/2}[1-(1-S_e^{1/m})^m]^2 \tag{9}$$

where $S_e=(\theta-\theta_r)/(\theta_s-\theta_r)$, θ_r is the residual (irreducible) water content, ψ is the suction head (a positive quantity), α and n are fitting parameters, and $m=1-1/n$.

The sorptivity, S, is estimated from the expression (Parlange, 1975)

$$S^2 = \int_{\theta_i}^{\theta_s}(\theta_s+\theta-2\theta_i)D(\theta)\mathrm{d}\theta \tag{10}$$

where $D(=K\mathrm{d}\psi/\mathrm{d}\theta)$ is the soil water diffusivity, which can be expressed as following for the van Genuchten–Mualem model

$$D = \frac{(1-m)K_s S_e^{1/2-1/m}}{\alpha m(\theta_s-\theta_r)}[(1-S_e^{1/m})^{-m}+(1-S_e^{1/m})^m-2] \tag{11}$$

The variable transformation of $\tilde{\theta}=\ln\{[(\theta_s-\theta_r)/(\theta-\theta_r)]^{1/m}-1\}$ is introduced to avoid an integration singularity at $\theta=\theta_s$ in (10). Substituting (8), (9) and (11) into (10) and using the new integration variable result in the following expression for S

$$S^2 = \frac{K_s\theta_s}{\alpha}\tilde{S}^2(m,\theta_s,\theta_r,\theta_i) \tag{12}$$

where

$$\begin{aligned}\tilde{S}^2(m,\theta_s,\theta_r,\theta_i) &= (1-m)\int_{-\infty}^{\tilde{\theta}_i}\left[1+\left(1-\frac{\theta_r}{\theta_s}\right)(e^{\tilde{\theta}}+1)^{-m}+\frac{\theta_r}{\theta_s}-\frac{2\theta_i}{\theta_s}\right]\\ &\times[(e^{\tilde{\theta}}+1)^{-m/2}e^{\tilde{\theta}(1-m)}+(e^{\tilde{\theta}}+1)^{-5m/2}e^{\tilde{\theta}(1+m)}\\ &-2(e^{\tilde{\theta}}+1)^{-3m/2}e^{\tilde{\theta}}]\mathrm{d}\tilde{\theta}\end{aligned} \tag{13a}$$

$$\tilde{\theta}_i = \ln\left[\left(\frac{\theta_s-\theta_r}{\theta_i-\theta_r}\right)^{1/m}-1\right] \tag{13b}$$

It can be shown that the dependence of the infiltration behavior on the residual and initial water content of the soil is relatively insignificant. While both the initial water content and the residual water content have relatively insignificant impact on the infiltration behavior, the initial water content has more significant influence. For example, for two sets of van Genuchten hydraulic parameters typical for sand and silty clay, to be given later, the difference of cumulative infiltration between using $\theta_r=0.1\theta_s$ and $\theta_r=0.4\theta_s$ is less than 1%. The difference of cumulative infiltration between using $\theta_i=0.1\theta_s$ and $\theta_i=0.4\theta_s$ is about 10%. In light of these results, we assume that the degree of relative residual and initial saturation is uniform across the field (i.e. θ_r and θ_i are fully correlated with the saturated water content θ_s), although some previous studies indicated that θ_r could be treated as a deterministic variable for loamy sand and was only slightly dependent on θ_s for sand (Warrick et al., 1977; Hopmans and Stricker, 1989). Given their relative insignificance on the infiltration behavior considered in this study, we could have assumed some deterministic values for θ_r and θ_i. Assuming a full correlation between θ_r (also θ_i) and θ_s could avoid an unrealistic possibility of θ_r or θ_i being greater θ_s in the generation of the random fields and would simplify our analysis. One can imagine that as the initial soil moisture increases, the infiltration will greatly diminishes. Therefore, the other condition implied in this study is that the initial soil condition should be in a relatively dry range. In summary, we consider three spatially variable fields: two soil hydraulic properties, δ and θ_s, and h_{surf} in relation to surface microtopography.

Field estimates of the scaling factor δ suggested that it is approximately lognormally distributed (Warrick et al., 1977; Russo and Bresler, 1980; Shouse and Mohanty, 1998). Based on the statistics of hydraulic parameters, the cross-correlated random fields of the input parameters are generated using the spectral method proposed by Robin et al. (1993). Random fields were produced with the power spectral density function, which was based on exponentially decaying covariance functions. The coherency spectrum, given by (14), is an indicator of parameter correlation,

$$R(\mathbf{f}) = \frac{\phi_{12}(\mathbf{f})}{[\phi_{11}(\mathbf{f})\phi_{22}(\mathbf{f})]^{1/2}} \tag{14}$$

where $\phi_{11}(\mathbf{f})$, $\phi_{22}(\mathbf{f})$ are the power spectra of the two random fields respectively, $\phi_{12}(\mathbf{f})$ is the cross-spectrum between the two random fields. The value of $|R|^2$ may range from 0 to 1, with $|R|^2=1$ (i.e. the correlation coefficient $\rho=1$ in the physical domain) indicating a perfect linear correlation between the random fields. Random fields of 10,000 nodes (on a 100×100 horizontal grid) are generated for $\ln(\delta)$, and $\ln(\theta_s)$ or $\ln(h_{surf})$, using the computer code of Robin et al. (1993).

4. Optimized *p*-order power and effective scaling factor

The 'effective' soil parameters of the heterogeneous soil formation are derived by conceptualizing the soil formation as an equivalent homogeneous medium. It requires that the 'effective' homogeneous soil will most closely discharge the ensemble-mean cumulative infiltration and produce the ensemble-mean surface flux.

The p-order power average (Korvin, 1982; Ababou and Wood, 1990; Gomez-Hernandez and Gorelick, 1989; Green et al., 1996) or p-norm $\hat{\xi}(p)$ for a set of N parameter values ξ is

$$\hat{\xi}(p) = \left[(1/N)\sum_{i-1}^{N}\xi_i^p\right]^{1/p} \tag{15}$$

The arithmetic ($p=1$), geometric ($p\to0$), and harmonic ($p=-1$) means are all particular cases of the power average.

The optimal values of p for various scenarios are obtained using an inverse procedure, which minimizes the following objective function

$$\text{obj} = \sum_{i-1}^{N}\left\{\frac{\hat{I}(i\Delta t)-\bar{I}(i\Delta t)}{\bar{I}(i\Delta t)}\right\}^2 + \sum_{i=1}^{N}\left\{\frac{\log[\hat{q}_s(i\Delta t)]-\log[\bar{q}_s(i\Delta t)]}{\log[\bar{q}_s(i\Delta t)]}\right\}^2 \tag{16}$$

where '–' denotes ensemble quantities (i.e. arithmetic averages), '^' indicates quantities calculated using a single set of parameter values corresponding to the optimal value of p ($\hat{p}$), Δt is the time step in our calculations, N is the number of total steps, and $T=N\Delta t$ is the total time range considered in the optimization. The objective function designated by (16) represents an equally weighted difference of cumulative infiltration and the logarithm (10-based) of the flux rate between the optimized values and the ensemble-mean values. We used this combination in defining the objective function mainly because total infiltration and the order of magnitude of surface flux are important components of subsurface interaction and water budget in large-scale hydrologic and global circulation models. It should be pointed out that the optimized parameter value depends on the total time range considered in the optimization (i.e. $T=N\Delta t$). We suggest a T range that should encompass the transition from early square root of time behavior (i.e. sorption) to the longtime traveling wave solution (i.e. infiltration). The $\hat{p}$ value that minimizes the above objective function represents an optimal value of p. The corresponding parameter values are the 'effective' parameters. The optimal p is the power that should be used in order to best simulate the ensemble behavior of heterogeneous soils. In other words, the optimal p is the power, which defines a best averaging scheme under the infiltration scenario considered in this study.

5. Results and discussion

For the reference values of the hydraulic parameters in dealing with heterogeneous soil hydraulic properties, we use some typical values of soil hydraulic parameters based on textural class from Schaap and Leij (1998). We selected two extreme textual classes, sand and silty clay, for our analysis. For sand, $\bar{k}_s=1624$(cm/day), $\bar{\alpha}=0.042$(1/cm) and $\bar{n}=3.44$. For silty clay, $\bar{k}_s=22.59$(cm/day), $\bar{\alpha}=0.042$(1/cm) and $\bar{n}=1.35$. Those values were calculated based on the statistic values given in Schaap and Leij (1998) and the assumption that these parameters are lognormally distributed.

In terms of the statistics of the random fields, a large range for the variance of the scaling factor was reported in the literature. The scaling factor derived from infiltration parameters for the R-5 watershed in Oklahoma had a mean of 1.0 and a standard deviation of 0.6 (Sharma and Luxmoore, 1979; Sharma et al., 1980). Warrick et al. (1977) reported the variance of

the scaling factor range from 0.23 to 3.29 for various soils. We used the scaling factor δ with a mean value equal to 1.0 and variance equal to 3.54, close to the upper end of the reported values for investigating its impact on the optimal effective power. The mean value for the saturated water content θ_s used in this study is 0.375 for sand and 0.481 for silty clay with a large variance of 1.02. Both δ and θ_s were assumed to be lognormally distributed. Since a relatively large variance was used for θ_s, a few values of the randomly generated θ_s values were larger than the maximum physically possible value of one (1) for the saturated water content θ_s. In our analysis, all the values of θ_s greater than 1 were replaced by 0.99. Therefore, the resulting lognormal distribution for θ_s is only approximate. Fig. 1 shows comparison of the actual distribution and the lognormal distribution for the saturated water content θ_s. Plotted in the same figure is the distribution of the scaling factor δ which is lognormal.

Before investigating the effects of parameter variabilities on the averaging scheme, it is useful to discuss the influence of individual parameters on the flow behavior at the local scale. In general, an increase in δ (related to hydraulic conductivity) increases the cumulative infiltration (water depth) and the flux. Increase in h_{surf} and θ_s also increases

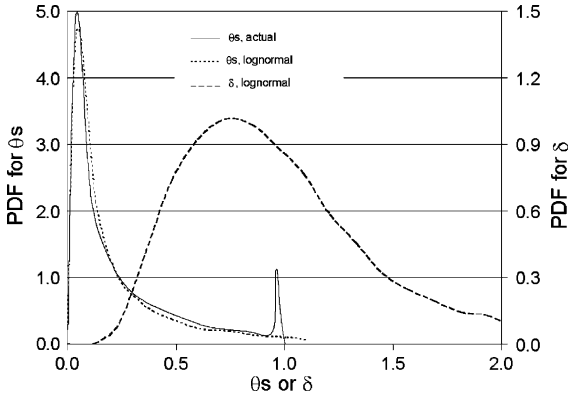

Fig. 1. Probability density functions (PDFs) for θ_s and δ. For θ_s, 'lognormal' distribution indicates the PDF based on the assumed lognormality while 'actual' distribution indicates the PDF for the θ_s field used in our calculations after assigning a value 0.99 for any values greater than 1. Both distributions shown have the same mean and standard deviation. For δ, the PDF is lognormal. Note the different ordinate scales for θ_s and δ.

cumulative infiltration and flux. Physically, higher microscopic characteristic length represents soil with larger mean pore size and therefore higher hydraulic conductivity. An increase in the cumulative infiltration and flux due to a larger ponding depth is physically obvious. It can be shown that the correlation among input parameters δ, θ_s, and h_{surf}, increases the variability of cumulative infiltration and the flux fields. The increased variability in the flux field due to correlation between δ and θ_s fields can be better understood by considering the separate effects of δ and θ_s on the flux and the implication of the correlation between δ and θ_s. A higher degree of correlation between δ and θ_s means that the values δ and θ_s in each cell would be either simultaneously high or low, thus augmenting the effect of each other and leading to increased flux variability across the cells. The same is also true for the correlation between δ and h_{surf} fields.

5.1. Sinusoidally varying ponding depth

First we consider a sinusoidal h_{surf} variation mimicking row/furrow based microtopography and randomly generated fields for δ and θ_s for a field-size of 800 m$\times$800 m. A row/furrow based microtopography and consequently the surface ponding depth was assumed to vary sinusoidally in the x direction according to the following function

$$h_{surf} = h_{avg}\left[1 + \sin\left(\frac{2\pi n_w x}{800}\right)\right] + h_1 \sin\left(\frac{2\pi n_{w1} x}{800}\right) \tag{17}$$

where h_{avg} is the average ponding depth. Eq. (17) simulates a microtopographical variation with two nested wave structures. For the columns in the x direction, the coordinates x_i are calculated as $x_i = 0.8i - 0.4$ for $i = 1,\ldots,100$. For any of the 100 rows in the y-direction, these x-coordinates are repeated. The first term in Eq. (17) indicates a sinusoidal variation with a wave number of n_w and an average ponding depth of h_{avg} over the entire pixel. The second term indicates another finer wave structure on top of the first one with a wave number of n_{w1} and amplitude of h_1. Fig. 2 shows some ponding scenarios with different combinations of various parameters in (17). Fig. 2a is for $h_{avg} = 0.1$ (m), $n_w = 10$ and $h_1 = 0$,

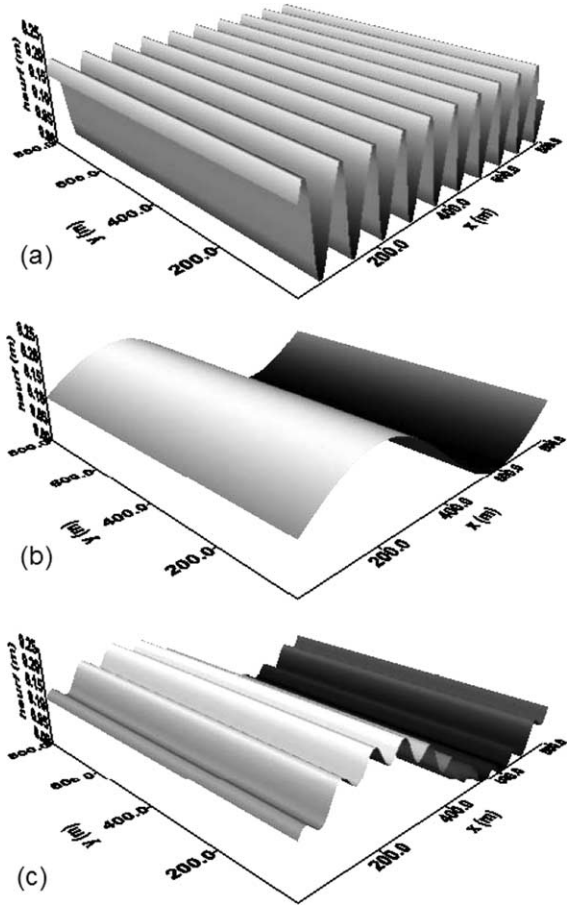

Fig. 2. Surface ponding scenarios: (a) $h_{avg}=0.1$ (m), $n_w=10$ and $h_1=0$, (b) $h_{avg}=0.1$ (m), $n_w=1$ and $h_1=0$, and (c) $h_{avg}=0.1$ (m), $n_w=1$, $h_1=0.25h_{avg}$, and $n_{w1}=10$.

indicating one wave structure with many wave numbers. An infinite wave number is equivalent to a uniform ponding depth. Fig. 2b is for $h_{avg}=0.1$ (m), $n_w=1$ and $h_1=0$, showing one wave structure and one wave number. Fig. 2c is for $h_{avg}=0.1$ (m), $n_w=1$, $h_1=0.25$ h_{avg}, and $n_{w1}=10$, expressing two wave structures.

Fig. 3 plots the cumulative infiltration as functions of time for sand (Fig. 3a) and silty clay (Fig. 3b), respectively. As we have mentioned earlier, the T range should encompass the transition from early square root of time behavior to the longtime traveling wave solution. For the sand parameters considered in this study, a T value of 75.6 (s) was considered appropriate, as seen in Fig. 3a where the transition

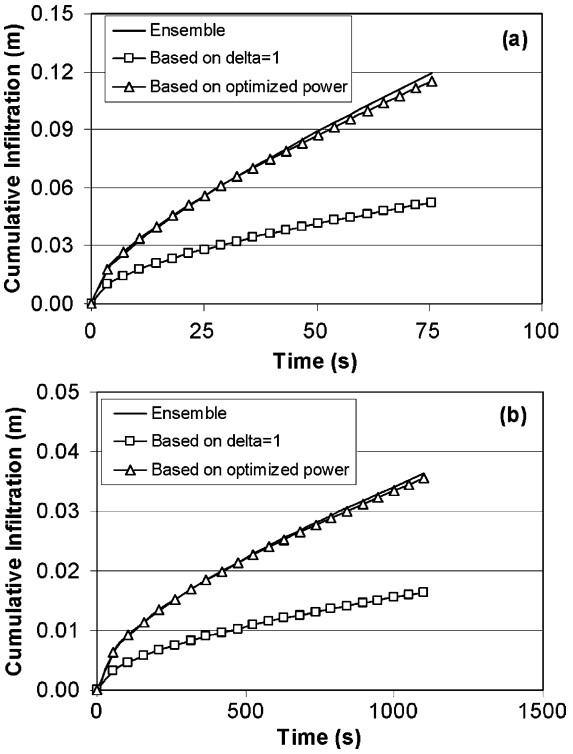

Fig. 3. Cumulative infiltration as functions of time: (a) for sand, and (b) for silty clay.

from sorption to infiltration is evident. For the silty clay, we estimate T based on the dimensionless time defined by Barry et al. (1995), $t^*=2t(K_s-K_i)^2/[S^2+2K_sh_{surf}(\theta_s-\theta)]$. For the case of small ponding depth, it can be approximated as $t^*=2t(K_s-K_i)^2/S^2$. That means for the same dimensionless time, the T ranges for sand and silty clay (sc) should be scaled according to $T_{sc}=T_{sand}[(K_s-K_i)^2_{sand}]/[(K_s-K_i)^2_{sc}$ $S^2_{sand}]$, which translates to $T_{sc}=1103.1$ (s). After this conversion, the infiltration behavior seen in Fig. 3a and b looks almost identical except the ranges in the abscissa and the ordinate. Plotted in Fig. 3 are the simulated results for the case of $h_{avg}=0.1$ (m), $n_w=10$, and $h_1=0.0$ when δ and θ_s are fully correlated (i.e. $|R|^2=1.0$). From Fig. 3, how the optimized power-averaging scheme improves over the simple arithmetic average (i.e. using $\delta=1$ or $p=1$) in terms of predicting the ensemble behavior of the heterogeneous soil is obvious. It can be seen that the results based on the arithmetic average severely underestimate the ensemble soil infiltration behavior.

5.1.1. Heterogeneous δ and homogeneous θ_s

Fig. 4 shows the optimal effective powers for the δ field (Fig. 4a) and the corresponding objective functions (Fig. 4b) when only δ is spatially variable in relation to the average ponding depths for a few selected surface topographic scenarios and soil textures. Generally, increasing ponding depth damps the variability effects, signified by a decreasing optimal effective power approaching a value of 1 (i.e. decreasing effective δ). Physically, ponding would reduce the effect of sorptivity variability, and increase the K_s varaibilty. Ponding has an overall damping effect probably because the increased K_s variability is not enough to offset the decreased sorptivity variability due to surface ponding. Large-scale topographic structure with no finer scale row/furrow structure (i.e. less frequent undulations) signified by small n_w enhance and augment the influence of ponding effects. The results for $n_w = 10$ are very close to those of uniform ponding, while the results for $n_w = 1$ are quite different. The finding is not surprising given the fact that a uniform ponding is equivalent to a limiting case of infinite wave number. For both sand and silty clay, second wave structure in ponding on top of the first has little effect on the optimal effective power. From Fig. 4b, it is more difficult to simulate the ensemble soil behavior using the effective parameter idea for the long wave (i.e. large structure) ponding scenario because the corresponding objective function is the largest. The optimal power value is generally larger than 1, suggesting that the effective scaling factor is greater than 1. In other words, the use of reference values for the hydraulic parameters would underestimate the surface flux rate and cumulative infiltration. Overall, the ensemble soil has higher infiltration rate irrespective of the textural composition.

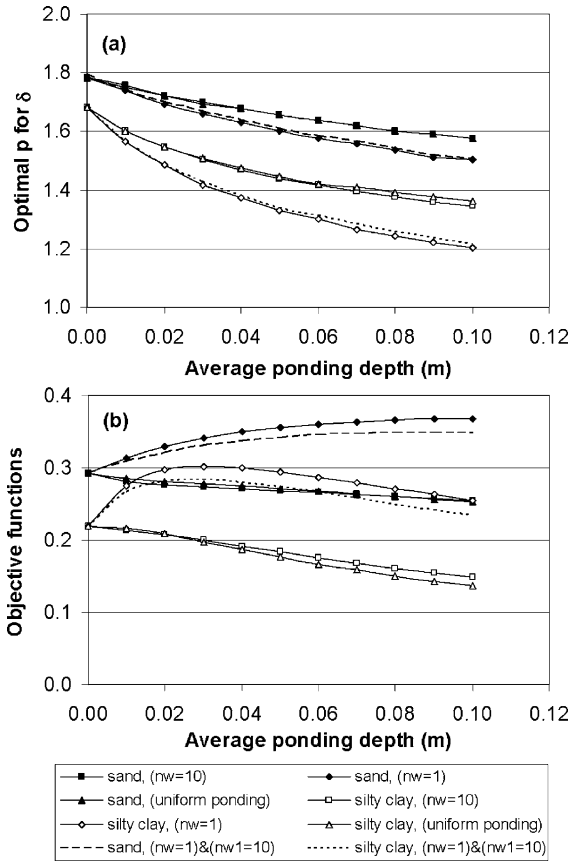

Fig. 4. Optimal effective powers for δ field and the corresponding objective functions vs. average ponding depths when only δ is heterogeneous: (a) optimal effective powers, and (b) objective functions.

5.1.2. Heterogeneous θ_s and homogeneous δ

Fig. 5 shows the optimal effective powers (Fig. 5a) and the corresponding objective functions (Fig. 5b) for θ_s field when only θ_s is spatially variable for a few selected surface ponding scenarios and soil textures. The optimal powers for θ_s field are generally between 0 and 1, suggesting that the effective θ_s is between geometric mean and arithmetic mean. It is easier to simulate the effect of heterogeneous θ_s since the corresponding objective functions are very small across different texture and topographic scenarios.

5.1.3. Heterogeneous δ and θ_s

When both input fields (δ and θ_s) are heterogeneous, it is found to be difficult to use an optimized effective θ_s since its spatial variability is relatively insignificant to influence the ensemble infiltration behavior as compared to the δ field. In this scenario, we suggest only to use the effective parameter idea for the δ field.

Fig. 6 plots the optimal powers for δ field (Fig. 6a) and the corresponding objective functions (Fig. 6b) vs. average ponding depths for a few surface ponding scenario and soil textures when δ and θ_s are fully correlated. As we have discussed previously, the spatial variability of the resulting surface flux and

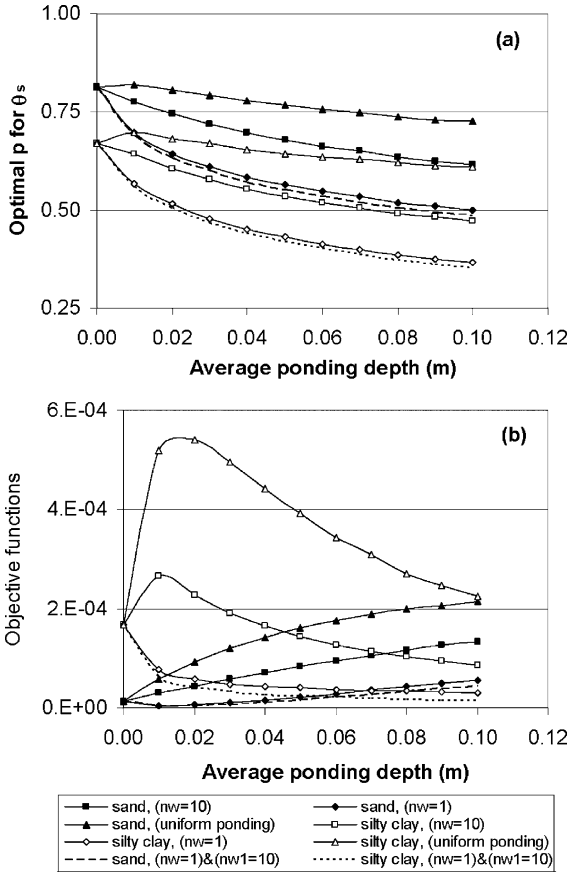

Fig. 5. Optimal effective powers for θ_s field and the corresponding objective functions vs. average ponding depths when only θ_s is heterogeneous: (a) optimal effective powers, and (b) objective functions.

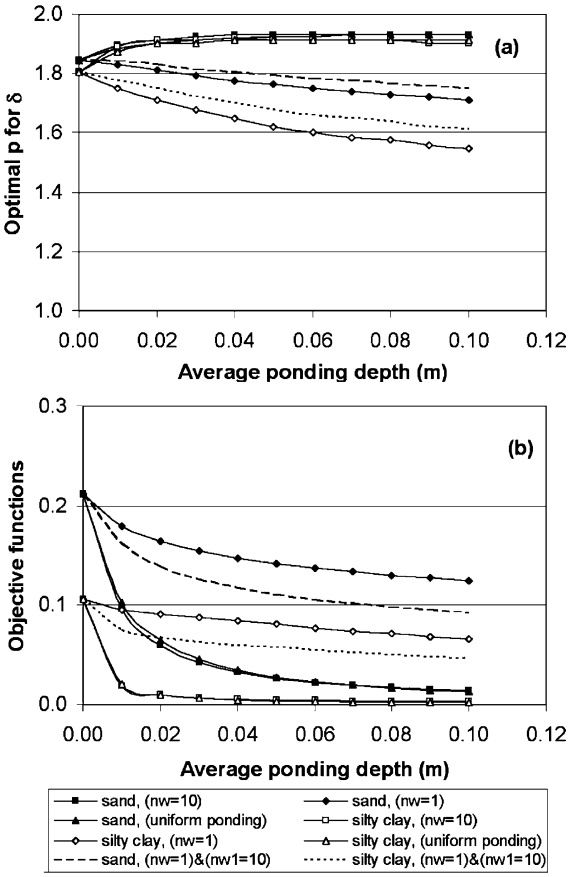

Fig. 6. Optimal powers for δ field and the corresponding objective functions vs. average ponding depths when δ and θ_s are fully correlated: (a) optimal effective powers, and (b) objective functions.

cumulative infiltration fields is enhanced by the correlation of the input heterogeneous fields. The optimal effective power results also reflect that trend, signified by larger optimal effective powers as compared to the single δ random field case shown in Fig. 4. However, note that the objective function values are smaller for the correlated case, meaning that the optimized effective average scheme captures the ensemble infiltration behavior of the heterogeneous soil more precisely for the correlated case. For comparison, Fig. 7 presents the optimal powers for δ field (Fig. 7a) and the corresponding objective functions (Fig. 7b) for the selected wave numbers of surface ponding and soil textures when δ and θ_s are uncorrelated. The results for both the effective optimal powers and the corresponding objective functions are very similar to those shown in Fig. 4, suggesting that the effects of the variable saturated water contents are indeed insignificant, as we have discussed.

For all the spatial variability scenarios discussed above, the optimal effective powers which can be used to best mimic the ensemble infiltration behavior for silty clay and sand vary in a relatively small range, with the optimal effective powers for silty clay being slightly smaller than those for sand.

5.2. Randomly varying ponding depth, h_{surf}

Given the relative insignificance of θ_s variability, next we fix the value of θ_s at its mean value and

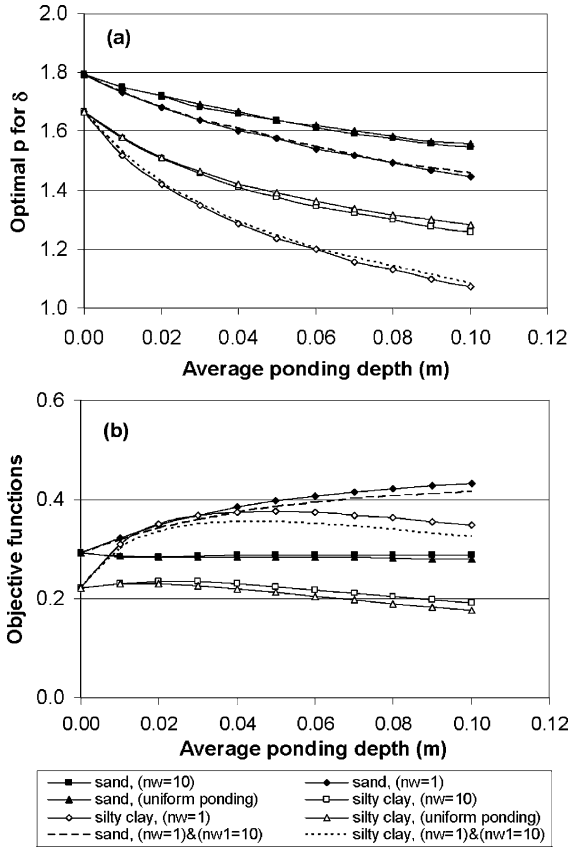

Fig. 7. Optimal powers for δ field and the corresponding objective functions vs. average ponding depths when δ and θ_s are uncorrelated: (a) optimal effective powers, and (b) objective functions.

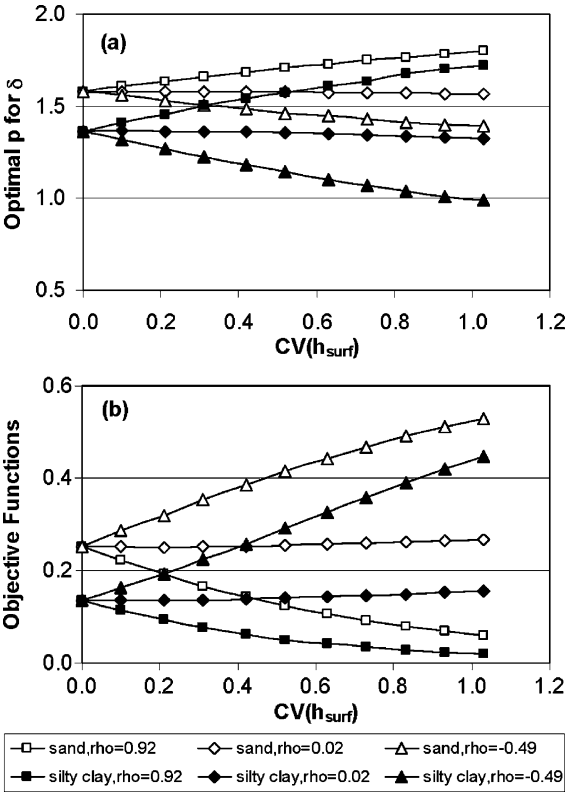

Fig. 8. Optimal powers for δ field and the corresponding objective functions vs. coefficient of variation of ponding depths: (a) optimal effective powers, and (b) objective functions. Note rho in the legend means the correlation between the δ and h_{surf} fields, ρ.

assume randomly δ and h_{surf} fields. The optimal effective powers for δ field (Fig. 8a) and the corresponding objective functions (Fig. 8b) in relation to the coefficient of variations for the ponding depths, h_{surf}, (i.e. CV(h_{surf}) in the figure) when the average ponding depth is 0.1 (m) at selected values of the correlation between the δ and h_{surf} fields (rho in the figure legend) are presented. In these simulations, the h_{surf} field has been assumed to obey the lognormal distribution, as opposed to the sinusoidal variations discussed previously. In general, an increased correlation between the δ and h_{surf} results in an increased optimal p, meaning an increased variability effect. In other words, a full correlation has the highest value for the optimal p and a fully negative correlation has the lowest value for the optimal p. This effect can also be explained by the individual effects of each parameter on the flow behavior. As explained earlier, a higher degree of correlation between δ and h_{surf} means that the values δ and h_{surf} in each cell would be either simultaneously high or low, thus augmenting the effect of each other and leading to increased flux variability across the cells. However, a highly correlated scenario can be more effectively simulated by the effective scaling factor, as can be evidenced by the smaller values of the objective functions (see Fig. 8b). It also means that the ensemble behavior of the heterogeneous soils can be simulated effectively by using arithmetic average ponding depth without affecting the effective scaling factor. In the case of uncorrelated scaling factor and the ponding depth ($\rho = 0.02$), the spatial variability of the ponding depth has little effect on the effective scaling factor, as can be seen from Fig. 8 which show little variation of both

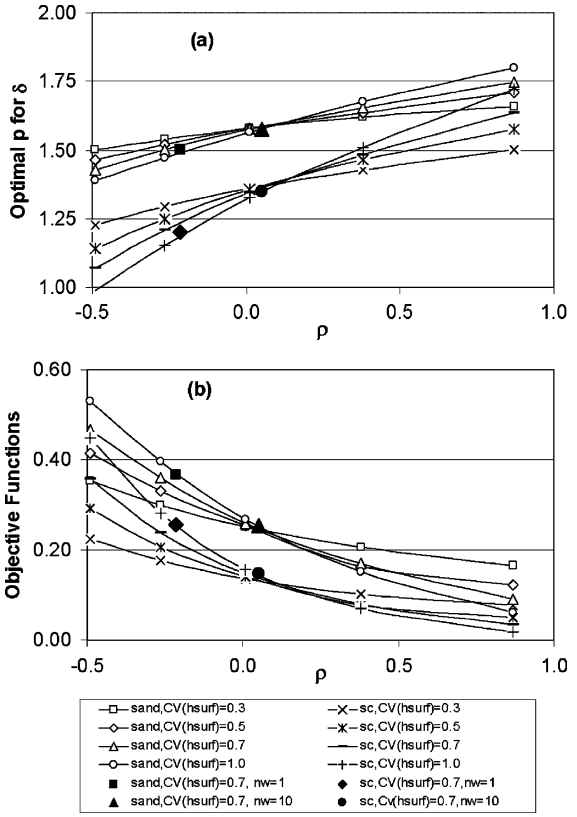

Fig. 9. Optimal powers for δ field and the corresponding objective functions vs. correlation between δ and h_{surf}, ρ: (a) optimal effective powers, and (b) objective functions.

the optimal p and the objective functions against the coefficients of variation for the ponding depth.

In Fig. 9, the optimal p for the scaling factor δ is plotted against the correlation between δ and h_{surf} fields (ρ) at selected coefficient of variations of the ponding depth for both sand and silty clay textures. An average value of 0.1 m for h_{surf} has been used for all scenarios including lognormally (open symbols) and sinusoidally (solid symbols) varying distributions of the ponding depth in Fig. 9. It can be observed that the sinusoidal ponding depth also follows the lead of random ponding depth despite of different distributions. Plotted in Fig. 10 are the probability distribution functions (PDFs) of the generated ponding depth field, h_{surf}, based on a lognormal distribution for both highly correlated and little correlated with the δ field, as well as sinusoidally varying ponding depth for both long ($n_w = 1$) and short

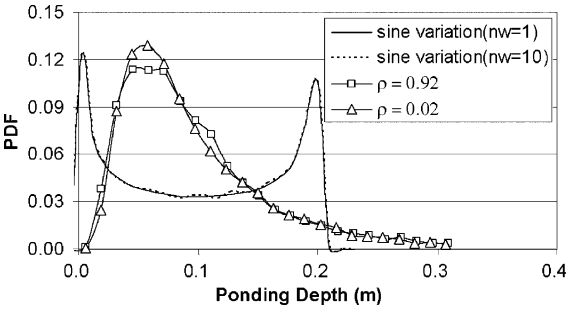

Fig. 10. Probability density functions (PDFs) of ponding depth for various scenarios.

($n_w = 10$) topographic structures. The PDFs for the sinusoidally varying ponding depth and the lognormally distributed ponding depth differ quite significantly. Also, the correlation between the δ field and the h_{surf}, ρ, does not alter the PDFs of the ponding depth. It however affects the optimal p for the δ field and the resulting objective functions (see Fig. 9). The difference in the wave number of the sinusoidal ponding depth variation does not change the PDFs of the ponding depth field, but it alters its correlation with the δ field. As a result, it also changes the optimal p for the δ field and the resulting objective functions (see Fig. 9). Therefore we may conclude that the correlation between the δ and the ponding depth fields is important for effective parameter estimation, while the effects of the PDFs of the ponding depth are secondary.

6. Concluding remarks

We used a relatively large variance (3.54) for the scaling factor and persistently demonstrated a narrow range of optimal p (between 1 and 2) for various soil and topographic scenarios and parameter correlations, while the possible value for p is between $-\infty$ and $+\infty$ and p should be equal to 1 when there is no variability (i.e. $\sigma_\delta^2 = 0$). We used two extreme soil textural classes (silty clay and sand) where parameters vary quite significantly. But these large ranges of mean do not result in a very large range for the optimal p either, which leads us to believe that the parameter mean and variance are not very important if we express our results in terms of p, instead of the actual effective parameter values. In view of the large

range of hydraulic properties for silty clay and sand and the large variabilities of the scaling factor considered in this study, a relatively small range in the optimal effective power values is somewhat encouraging with regard to effective parameter estimation for large land areas encompassing various soil textures, large/small topographic structures and other hydrologic scenarios.

Variability in the scaling factor has much more significance on the ensemble behavior than that in the saturated water content and the ponding depth. The coupled effects of these two random fields can be simulated by optimizing the power for the scaling factor alone, while the lone effects of θ_s variability can be precisely simulated by using a power for the θ_s field between 0 and 1 (i.e. between geometric mean and arithmetic mean). The effects of the variable saturated water contents are most significant when their spatial variation is correlated with the spatial variation of the scaling factor, where the correlation will enhance soil heterogeneity behavior. Generally, surface ponding has the effects of suppressing the heterogeneity, signified by a decreasing effective optimal power (i.e. decreasing effective δ).

A secondary topographic structure in surface ponding on top of the first larger-scale structure has little effect on the optimal effective power. The correlation between the scaling factor and the saturated water content increases the soil heterogeneous effects, indicated by the increased variability of the surface flux and cumulative infiltration fields and the increased optimal effective powers for simulating the ensemble behavior of infiltration. However, the ensemble behavior can be more precisely mimicked through the idea of optimal effective powers, signified by the smaller objective functions as compared to the uncorrelated case.

The correlations among parameters augment the heterogeneous effects, which require larger values for the scaling factor p-norm.

Acknowledgements

This project is supported by NASA (grant nos. NAG5-8682 and NAG5-11702) and NSF-SAHRA. The study is also supported in part by the Water Resources Research Act, Section 104 research grant program of the U.S. Geological Survey.

References

Ababou, R., Wood, E.R., 1990. Comments on 'Effective groundwater model parameter values: influence of spatial variability of hydraulic conductivity, leakage, and recharge' by J.J. Gomez-Hernandez, S.M. Gorelick. Water Resour. Res. 26 (8), 1843–1846.

Barry, D.A., Parlange, J.-Y., Haverkamp, R., Ross, P.J., 1995. Infiltration under ponded conditions: 4. An explicit predictive infiltration formula. Soil Sci. 160 (1), 8–17.

Brooks, R.H., Corey, A.T., 1964. Hydraulic Properties of Porous Media. Colorado State Univ. pp. 27 (Hydrology Paper No. 3).

Ferrante, M., Yeh, T.-C.J., 1999. Head and flux variability in heterogeneous unsaturated soils under transient flow conditions. Water Resour. Res. 35 (5), 1471–1480.

Green, T.R., Contantz, J.E., Freyberg, D.L., 1996. Upscaled soil–water retention using van Genuchten's function. J. Hydrologic Eng., ASCE 1 (3), 123–130.

Gomez-Hernandez, J.J., Gorelick, S.M., 1989. Effective groundwater model parameter values: influence of spatial variability of hydraulic conductivity, leakage, and recharge. Water Resour. Res. 25 (3), 405–419.

Haverkamp, R., Parlange, J.-Y., Starr, J.L., Schmitz, G., Fuentes, C., 1990. Infiltration under ponded conditions: 3. A predictive equation based on physical parameters. Soil Sci. 149 (5), 292–300.

Hopmans, J.W., Schukking, H., Torfs, P.J.J.F., 1988. Two-dimensional steady state unsaturated water flow in heterogeneous soils with autocorrelated soil hydraulic properties. Water Resour. Res. 24 (12), 2005–2017.

Hopmans, J.W., Stricker, J.N.M., 1989. Stochastic analysis of soil water regime in a watershed. J. Hydrol. 105, 57–84.

Jury, W.A., Russo, D., Sposito, G., 1987. The spatial variability of water and solute transport properties in unsaturated soil, II. Scaling models of water transport. Hilgardia 55, 33–57.

Kim, C.P., Stricker, J.N.M., 1996. Influence of spatially variable soil hydraulic properties and rainfall intensity on the water budget. Water Resour. Res. 32 (6), 1699–1712.

Kim, C.P., Stricker, J.N.M., Feddes, R.A., 1997. Impact of soil heterogeneity on the water budget of the unsaturated zone. Water Resour. Res. 33 (5), 991–999.

Kim, C.P., Stricker, J.N.M., Torfs, P.J.J.F., 1996. An analytical framework for the water budget of the unsaturated zone. Water Resour. Res. 32 (12), 3475–3484.

Korvin, G., 1982. Axiomatic characterization of the general mixture rule. Geoexploration 19, 267–276.

Mayer, A.S., Miller, C.T., 1996. The influence of mass transfer characteristics and porous media heterogeneity on nonaqueous phase dissolution. Water Resour. Res. 32 (6), 1551–1567.

Miller, E.E., 1980. Similitude and scaling of soil water phenomena. In: Hillel, D. (Ed.), Application of Soil Physics. Academic Press, New York, pp. 300–318.

Miller, E.E., Miller, R.D., 1956. Physical theory of capillary flow phenomena. J. Appl. Phys. 27, 324–332.

Milly, P.C.D., Eagleson, P.S., 1987. Effects of spatial variability on annual average water balance. Water Resour. Res. 23 (11), 2135–2143.

Montoglou, A., Gelhar, L.W., 1987. Stochastic modeling of large-scale transient unsaturated flow systems. Water Resour. Res. 23 (1), 37–46.

Montoglou, A., Gelhar, L.W., 1987. Capillary tension head variance, mean soil moisture content, and effective specific soil moisture capacity of transient unsaturated flow in stratified soils. Water Resour. Res. 23 (1), 47–56.

Montoglou, A., Gelhar, L.W., 1987. Effective hydraulic conductivities of transient unsaturated flow in stratified aquifer. Water Resour. Res. 23 (1), 57–67.

Parlange, J.-Y., 1975. On solving the flow equation in unsaturated soils by optimization: horizontal infiltration. Soil Sci. Soc. Am. Proc. 39, 415–418.

Parlange, J.-Y., Haverkamp, R., Touma, J., 1985. Infiltration under ponded conditions: 1. Optimal analytical solution and comparison with experimental observations. Soil Sci. 139 (4), 305–311.

Robin, M.J.L., Gutjahr, A.L., Sudicky, E.A., Wilson, J.L., 1993. Cross-correlated random field generation with the direct Fourier transform method. Water Resour. Res. 29 (7), 2385–2397.

Russo, D., 1991. Stochastic analysis of simulated vadose zone solute transport in a vertical cross section of heterogeneous soil during nonsteady water flow. Water Resour. Res. 27 (3), 267–283.

Russo, D., Bresler, E., 1980. Scaling soil hydraulic properties of a heterogeneous field. Soil Sci. Soc. Am. J. 44, 681–684.

Schaap, M.G., Leij, F.J., 1998. Database-related accuracy and uncertainty of pedotransfer functions. Soil Sci. 163, 765–779.

Sharma, M.L., Gander, G.A., Hunt, C.G., 1980. Spatial variability of infiltration in a watershed. J. Hydrol. 45, 101–122.

Sharma, M.L., Luxmoore, R.J., 1979. Soil spatial variability and its consequences on simulated water balance. Water Resour. Res. 15, 1567–1573.

Shouse, P.J., Mohanty, B.P., 1998. Scaling of near-saturated hydraulic conductivity measured using disc infiltrometers. Water Resour. Res. 34, 1195–1205.

Sposito, G., Jury, W.A., 1985. Inspectional analysis in the theory of water flow through unsaturated soil. Soil Sci. Soc. Am. J. 49, 791–798.

Unlu, K., Nielsen, D.R., Beggar, J.W., 1990. Stochastic analysis of unsaturated flow: one-dimensional Monte Carlo simulations and comparisons with spectral perturbation analysis and field observations. Water Resour. Res. 26 (9), 2207–2218.

Warrick, A.W., Mullen, G.J., Nielsen, D.R., 1977. Scaling field-measured soil hydraulic properties using a similar media concept. Water Resour. Res. 13 (2), 355–362.

Zhu, J., Mohanty, B.P., 2002. Spatial averaging of van Genuchten hydraulic parameters for steady state flow in heterogeneous soils. Vadose Zone Journal 1, 261–272.